

# Uniaxial electromechanical behavior of ferroelectric ceramic PZT-53

Q. WAN, C. CHEN\*, Y. P. SHEN\*

*The State Key Laboratory, School of Civil Engineering and Mechanics, Xi'an Jiaotong University, Xi'an, 710049, People's Republic of China*

*E-mail: CChen@mail.xjtu.edu.cn*

*E-mail: YPShen@mail.xjtu.edu.cn*

**Published online:** 17 January 2006

Effect of compressive pre-stress and biased electrical field on the uniaxial electromechanical behavior of a soft ferroelectric ceramic PZT-53 is investigated. The emphasis is on the effect of electric and mechanical loading history upon the response of PZT-53 to external loading and on the effect of pre-stress and biased electrical field upon the electro-mechanical coupling behavior. It is found that the uniaxial behavior of the PZT-53 is sensitive to the compressive pre-stress and biased electrical field, and is less sensitive to the loading history. Obtained results are expected to shed insightful light on developing reliable constitutive model for ferroelectric ceramics. © 2006 Springer Science + Business Media, Inc.

## 1. Introduction

Ferroelectric ceramic PZT are widely used as electromechanical sensor, transducers and actuators [1–3] due to their superior piezoelectric coupling property and high Curie temperature. The PZT family can be roughly classified into two groups: “hard” and “soft”. The materials are doped with small amounts of substitutional materials to soften them (donor, usually niobium) or harden them (acceptor, usually iron). Soft PZT has lower coercive field, higher piezoelectric coefficients, and higher dielectric loss. Hard PZT has higher coercive field (most hard compositions must be poled at elevated temperatures to increase domain wall mobility), lower piezoelectric coefficients and lower dielectric loss.

Many advanced applications of PZT require either large actuation displacement or large driving force. Such conditions may cause nonlinearity, as well as permanent deformation of the ferroelectric materials and also the attached metallic electrodes, deteriorating the material and structural performance [4–6]. The nonlinearities are most pronounced in the vicinity of defects with stress concentration, e.g., the electrode edges and flaws [7], which may be present either in the ferroelectric or at the ferroelectric(electrode interface). A thorough understanding of the highly nonlinear constitutive behavior of ferroelectric materials is thus essential to guarantee the success of their applications. To this end, a number of constitutive models for ferroelectric ceramics have been developed (see, [8–

11] for example), with varying complexity and success. In order to assess these constitutive models, a systematic experimental study of the electromechanical behavior of ferroelectric ceramics is necessary. Most available experiment studies are on the uniaxial electromechanical response of PZT ceramics, e.g., the uniaxial stress-strain response of PZT investigated by Cao and Evans [12] and by Schaufele and Hardtl [13], and the coupled electromechanical hysteresis behavior of a PLZT ceramic [8, 10, 11]. By contrast, only limited results are available on the multi-axial behavior of ferroelectric ceramics. Chen and Lynch [14] investigated the “yield surface” of ferroelectric ceramics under proportional biaxial stressing. Huber and Fleck [15] and Shieh *et al.* [18] studied the response of PZT to multi-axial electric loading and obtained the initial “electric yield surface”. Moreover, it is of theoretical and practical importance to explore the effect of loading history and biased stress and electric field on the constitutive behavior of ferroelectric ceramics, in order to provide an unambiguous picture of the electromechanical behavior of ferroelectric ceramics. Such effects on the complex constitutive ferroelectric materials (except for Refs. 10 and 11, which focus mainly on the effect of biased stressing on the uniaxial electromechanical behavior of PLZT) have yet to be thoroughly investigated.

Inspired by these considerations, the aim of this study is to investigate the effect of loading history,

\* Author to whom all correspondence should be addressed.

compressive pre-stress and biased electric field on the uniaxial electromechanical response of PZT-53. In addition, the effects of the frequency of the applied electric field on the response have also been studied.

## 2. Experiment

The materials used in this study are typical soft ferroelectric ceramic PZT-53 which has a Zr/Ti ratio of approximately 53/47. Each grain of the poled ceramic is a single crystal with a tetragonal perovskite structure at room temperature. The plate specimens of nominal dimensions  $10 \times 10 \times 5$  mm were cut from a PZT-53 batch of the same thickness 5 mm using a diamond saw. The specimen top and bottom major surfaces were electroded with sputtered Ag. The sharp edges and corners of all specimens were slightly rounded to prevent chipping, stress concentration, and cracking upon loading. To avoid bending stress and inhomogeneous distribution of stress during loading, it is important to maintain that the top and bottom faces of the Brass blocks of the loading grips and those of specimens are parallel (see Fig. 1). To this end, all specimens are polished again after two major surfaces are electroded. It should be noted that, in general, flat specimens (e.g., those used here) are not suitable for compression testing due to the effect of friction between specimen and load grips. However, the top and bottom surfaces of the specimens used in this study are sputtered with Ag, which has a small friction coefficient and can significantly reduce the frictions between specimen and load grips. Moreover, the surfaces of the load grips used in this study (i.e., the brass shown in Fig. 1) have been carefully polished, which can further diminish the friction. In fact, our results (as shown later) on the effects of compressive stress on the electric displacement and strains curves are qualitatively similar to those reported by Ref. 10 where long specimens of dimensions  $5 \times 5 \times 15$  mm are used. We conclude that the size effect of the specimens used in this study on the mea-

sured results is small. Strain gauges with gauge size  $0.3 \times 1.8$  mm and matrix size  $2.7 \times 2.7$  mm bonded on the side surfaces perpendicular to the major surfaces are used to measure the strains in the thickness direction and its transverse direction, respectively. In order to check whether the specimen deforms uniformly, two pairs of strain gauges are bonded to the side surfaces opposite to each other. It is expected that each pair of strain gauges shall output nearly the same reading provided that the specimen deforms uniformly. In this study, it is found that uniform deformation can be guaranteed by careful test preparation. Nevertheless, the average reading of each pair of strain gauges is reported in the following.

The experimental setup shown in Fig. 1 is adapted from Huber and Fleck [15] and Shieh *et al.* [18], allowing for simultaneously applying uniaxial electric field and stress to the specimen. A servo-hydraulic test frame applies the compressive load whilst the electric field is provided by a high voltage amplifier. The sample with attached strain gauges is placed in an oil bath to prevent high voltage arcing. Ethoxylene blocks are used to electrically isolate the sample from the test frame. Brass blocks are attached to the high voltage amplifier. For alignment, the specimen is carefully centered between the brass blocks and a steel spherical alignment fixture to accommodate slight misalignment of the specimen. The stress is calculated from the force and the cross sectional area of the specimen. The charge per unit area on the electrode is equal to the normal component of the electric displacement, and is measured by monitoring the voltage of a capacitor ( $93.95 \mu\text{F}$ ) connected from the bottom electrode of the specimen to the ground. A high voltage is connected to the top electrode of the specimen. Output of the instrumented system is recorded by a computer through a multiple-channel analog to digital converter.

## 3. Results and discussions

Before proceeding to carry out systematic experiment study, it is necessary to choose an appropriate frequency of the applied electric field to mimic the quasi-static loading which is of interest in this study. We consider a polarized PZT-53 ceramic sample subjected to electric field of triangular waveform with magnitude being 1.56kV/mm. Several frequencies (0.01, 0.02, 0.04, and 0.16 Hz) of the electric field are considered. Obtained results show that the results for 0.01 and 0.02 Hz are virtually the same and they are slight different from those for electric field with frequency 0.04 and 0.16 Hz (see, Fig. 2 for the  $E_3-P_3$  and  $E_3-\varepsilon_3$  curves). Therefore, electric field of triangular waveform and frequency 0.02 Hz is applied in the following to mimic quasi-static electric loading.

### 3.1. $E_3-P_3$ , $E_3-\varepsilon_{33}$ and $E_3-\varepsilon_{11}$ response loops under compressive pre-stress

We examine first the effect of constant compressive pre-stress upon the uniaxial electromechanical response of PZT-53. The loading history is shown in Fig. 3: a sequence

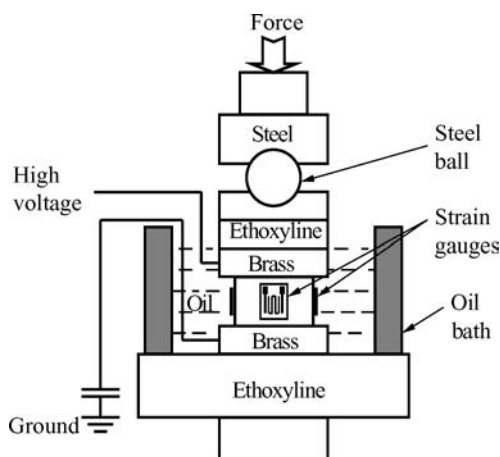


Figure 1 Sketch of the electro-mechanical loading system. The specimen is immersed in oil bath. A servo-hydraulic test frame applies the force with the high electric field provided by a high voltage amplifier.

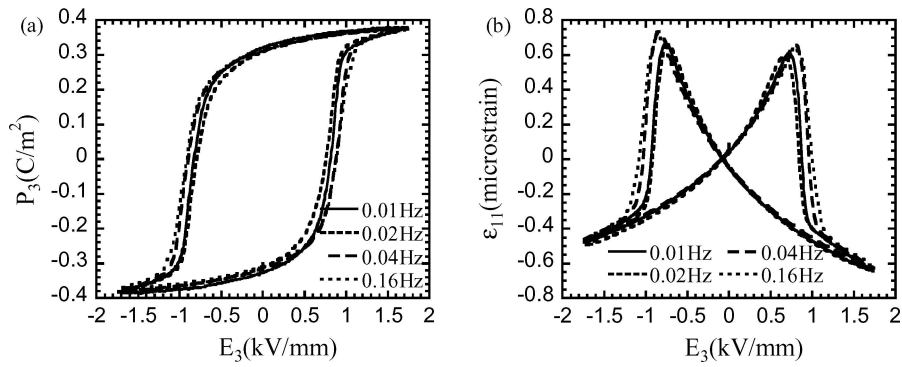


Figure 2 Effect of the frequency of the applied triangular electric field upon the  $E_3 - P_3$  and  $E_3 - \varepsilon_{33}$  curves of PZT-53.

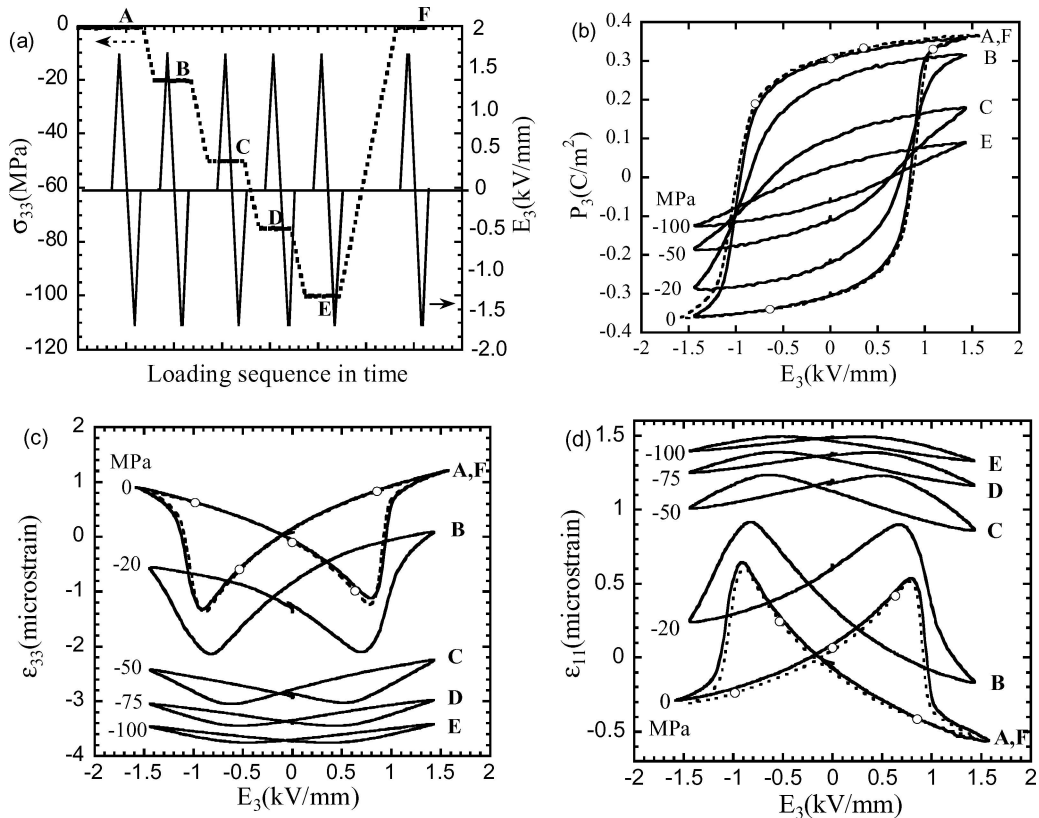


Figure 3 (a) The loading history, and (b)–(d) the  $E_3 - P_3$ ,  $E_3 - \varepsilon_{33}$  and  $E_3 - \varepsilon_{11}$  loops with various constant compressive pre-stresses A–F shown in Fig. 3(a).

of constant compressive stress  $\sigma_{33}$  ( $\sigma_{33} = 0, 20, 50, 75, 100, 0$  MPa, indicated by A–F in Fig. 3a, respectively) was imposed to the specimen in the poling direction; at each level of the applied constant compressive loading the specimen was simultaneously subjected to a triangular electric field  $E_3$  of magnitude 1.56 KV/mm and frequency 0.02 Hz. The  $E_3 - P_3$ ,  $E_3 - \varepsilon_{33}$  and  $E_3 - \varepsilon_{11}$  loops corresponding to various pre-stresses (A–E) are shown in Figs. 3b–d. Note from Fig. 3a that two sets of experiments were conducted for the case  $\sigma_{33} = 0$  (i.e., A and E): one at the beginning of the loading history and one at the end of the loading history. As mentioned before, this is to investigate whether the history of loading affects the material behavior.

It can be seen from Figs. 3b–d that the  $E_3 - P_3$ ,  $E_3 - \varepsilon_{33}$  and  $E_3 - \varepsilon_{11}$  response loops of PZT-53 are very sensitive to the constant compressive pre-stress: the sizes of the observed response loops are reduced by the presence of the pre-stress; the slopes of the  $E_3 - \varepsilon_{33}$  and  $E_3 - \varepsilon_{11}$  curves at  $E_3 = 0$  (normally referred to as the piezoelectric coefficient  $d_{333}$  and  $d_{311}$  when  $\sigma_{33} = 0$ ) decrease with pre-stress increasing.

Dependence of the coercive electric field  $E_c$  (electrical field at zero polarization) and remnant polarization  $P_r$  (polarization at zero electrical field) upon the applied compressive pre-stress can be inferred from Fig. 3a (see, Fig. 4). It is noticed from Fig. 4 that both the coercive field and the remnant polarization decrease with increasing the

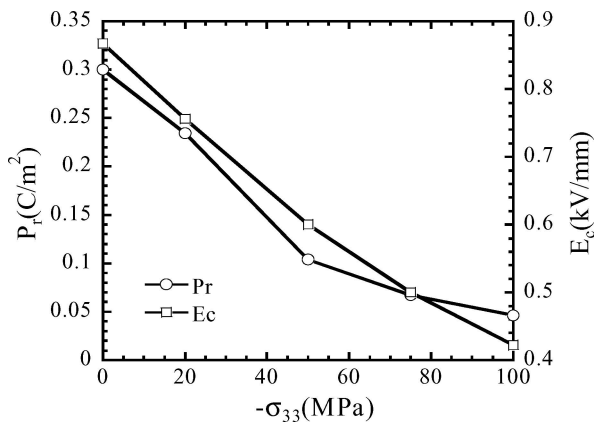
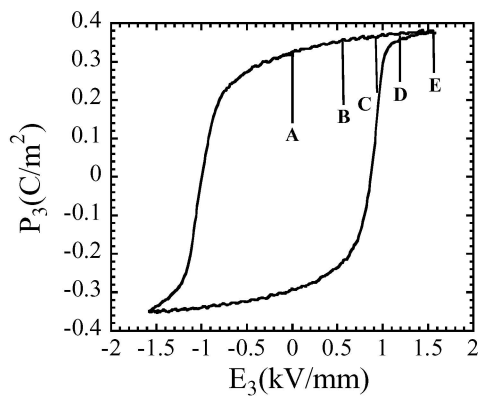


Figure 4 Effect of compressive constant pre-stress on the coercive electric field  $E_c$  and remnant polarization  $P_r$ .

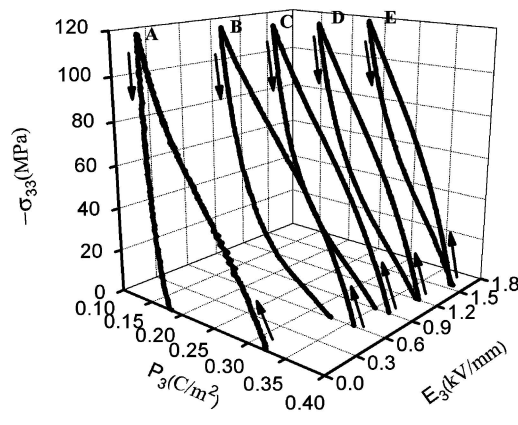
magnitude of the compressive stress. Such feature can be explained as follows.

When the compressive stress parallel to the poling direction is applied to the polarized PZT-53 plate, it induces  $90^\circ$  domain switching and significant strain mismatch.

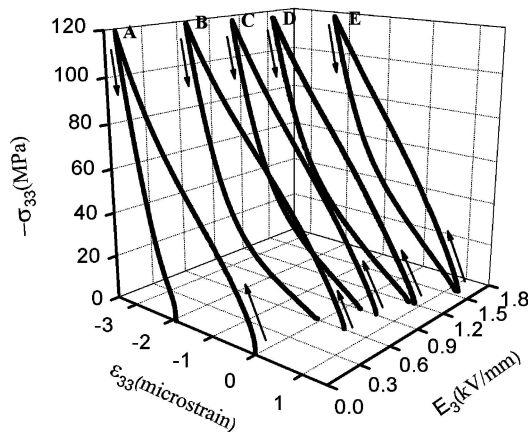
Usually, strain mismatch leads to internal stress and internal energy in the material: the bigger the magnitude of the compressive stress, the greater the resulted internal stress and energy. The high internal energy de-stabilizes the domains. Therefore, electric field driven domain switching becomes easier when the constant compressive stress is simultaneously present, i.e., the coercive field decreases with increasing the magnitude of the compressive stress. Similar finding has been revealed by Lynch [11], Zhou *et al.* [10] and Fang and Li [16]. Fang and Li also proposed a model for the diminishing of coercive field with increasing the biased stress. The effect of the presence of constant compressive pre-stress on the domain switch is two-fold, however. It renders it easier for the domain switching to start due to the high internal stress and energy; at the same time, it makes vast domains perpendicular to the compression direction hardly switch to the direction along the compressive stress completely. This is confirmed by the results shown in Fig. 3c–d, which show that the aggregate of strain (defined as the difference between the maximum and minimum strain for a complete responsive loop) during each electric loading



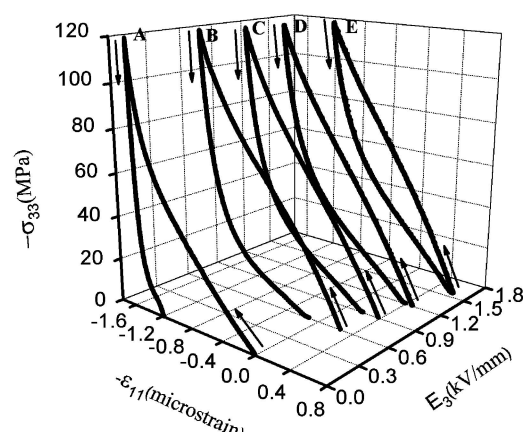
(a)



(b)



(c)



(d)

Figure 5 (a) The biased constant electric fields considered in this study are marked on a  $E_3 - P_3$  curve with  $\sigma_{33} = 0$  as straight lines (A–E). (b)–(d) The  $P_{33} - \sigma_{33}$ ,  $\epsilon_{33} - \sigma_{33}$  and  $\epsilon_{11} - \sigma_{33}$  curves of PZT-53 subjected to uniaxial compressive loading and unloading and different biased constant electric fields marked in Fig. 5(a) as A–E.

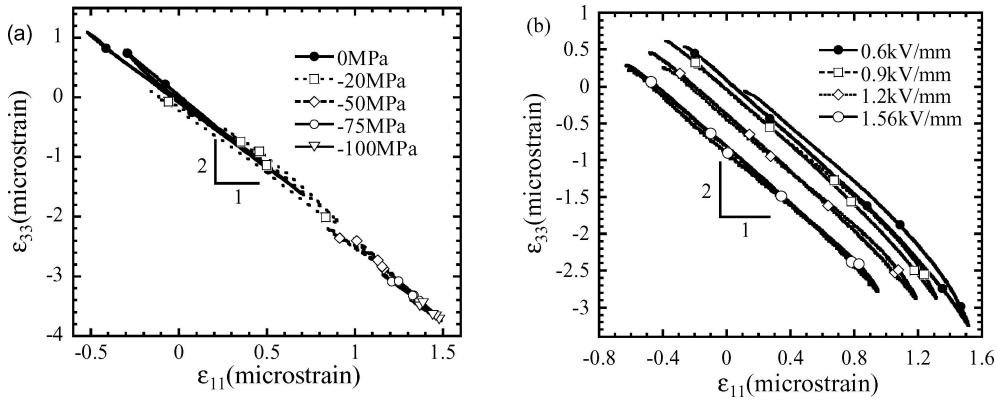


Figure 6 (a) and (b): The  $\varepsilon_{33} - \varepsilon_{11}$  curves corresponding to Figs 3 and 5, respectively.

cycle becomes less with increasing the magnitude of the compressive stress. A direct consequence of the incompleteness of the domain switching is that the magnitude of polarization change (and also the remnant polarization) is reduced by the applied compressive stress during the electric loading cycle (see Figs 3b and 4b).

Another important conclusion drawn from Fig. 3 is that after a sequence of loading with various pre-stress levels, the  $E_3 - P_3$ ,  $E_3 - \varepsilon_{33}$  and  $E_3 - \varepsilon_{11}$  loops at  $\sigma_{33} = 0$  MPa are almost identical to those at the beginning of the loading (compare the results labeled by A and F), implying that load history doesn't significantly affect the behavior of PZT-53. A detailed study on this issue will be shown in Section 3.3.

### 3.2. Uniaxial response under biased constant electric field

The effect of biased constant electric field upon the uniaxial electromechanical response of PZT-53 to external compressive stressing has also been studied. The biased electric fields associated with the compressive loading-unloading cycles are labeled on a  $P_{33} - E_{33}$  curve with  $\sigma_{33} = 0$  (see, Fig. 5a) to show the magnitude of the biased electric field relative to that of the coercive electric field, with cases A-E corresponding to electric field of magnitude being 0, 0.6, 0.9, 1.2, 1.56 kV/mm, respectively. Experiment of each loading and unloading cycle with varying biased electric field levels is conducted as follows. The specimen is first fully poled at high electric field to ensure a full polarization state at the beginning of each loading cycle. The electric field is then lowered from the high electric field and held at a constant value. Subsequently, a uniaxial compressive stress is ramped to  $-120$  MPa from a small compressive stress ( $-0.4$  MPa) at the rate of 10 MPa/min, then back to  $-0.4$  MPa at 20 MPa/min (a loading-unloading cycle). The small compressive stress ( $-0.4$  MPa) rather than zero is used to keep the specimen at the same position for each loading cycle. Each loading and unloading cycle took about 18 min to complete.

Fig. 5b shows the measured  $P_3 - \sigma_{33}$  curves for different magnitudes of biased constant electric field. The initial polarizations at the beginning of each loading-unloading cycle are consistent with those presented in Fig. 5a, giving 0.324, 0.358, 0.369, 0.376, 0.381 C/m<sup>2</sup> for the cases A–E, respectively. It is seen from Fig. 5b that, for the case without biased constant electric field, the compressive loading-unloading induces significant domain switching, which is evident from the un-recovered polarization (i.e., the difference between the polarizations at the end and the beginning of the loading-unloading cycle). Specifically, under zero electric field, 90° domain switching and depolarization occur when the compressive loading stress exceeds  $-10$  MPa (the polarization changing from 0.324 to 0.13 C/m<sup>2</sup>). During unloading from  $-120$  MPa to  $-0.4$  MPa, there is little re-polarization (the polarization varying from 0.13 to 0.165 C/m<sup>2</sup>). The un-recovered polarization for the loading-unloading cycle in the case of vanished electric field is thus equal to 0.159 C/m<sup>2</sup>. It is further noted the un-recovered polarization and hysteresis diminishes with increasing the magnitude of the biased constant electric field, implying that the biased electric field hampers the domain switching during the compressive loading and increases the domain back switching during the compressive unloading. The feature of decreased

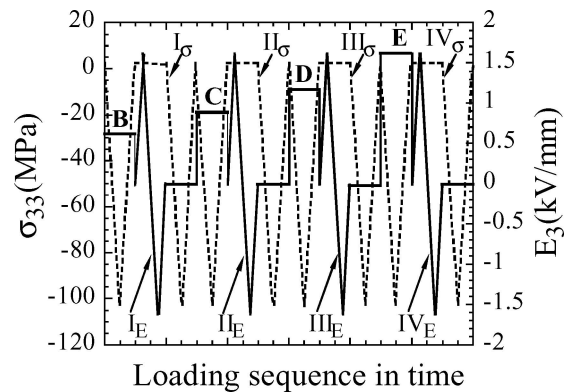


Figure 7 Sketch of the loading history. Broken line denotes compressive stress loading, and solid line refers to electrical loading. Letters B–D correspond to those shown in Fig. 5.

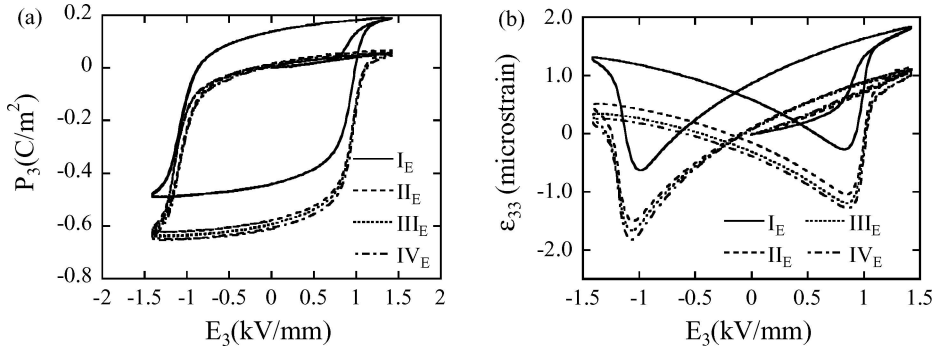


Figure 8 The  $E_{33} - P_3$  and  $E_3 - \varepsilon_{33}$  curves of PZT-53 for four different electric loading cycles (labeled as  $I_E - IV_E$  in Fig. 7) during a series of combined electric-mechanical loadings.

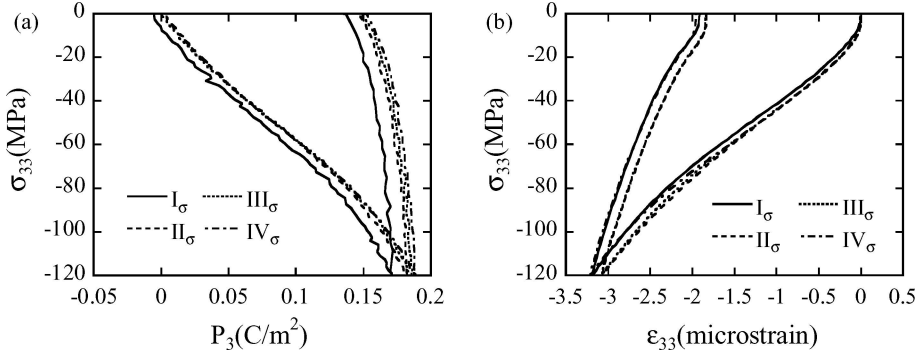


Figure 9 The  $P_3 - \sigma_{33}$  and  $\varepsilon_{33} - \sigma_{33}$  curves of PZT-53 for four different uniaxial compressive loading cycles (labeled as  $I_\sigma - IV_\sigma$  in Fig. 7) during the interval of a sequence of combined electric-mechanical loadings.

hysteresis with increasing the biased constant electric field has also been observed in Figs 5c and d for the strain-stress curves. Such characteristic can be understood by noting that since the biased constant electric field is in the same direction as that of the polarization it actually enforces the polarization and makes it difficult to depolarization during the loading-unloading cycle.

It is interesting to re-draw the results of Figs. 3c–d and 5c–d in the transverse strain ( $\varepsilon_{11}$ )-longitudinal strain ( $\varepsilon_{33}$ )space, presented in Fig. 6a and b, respectively. The slope of  $-2$  for all the  $\varepsilon_{11} - \varepsilon_{33}$  curves of PZT-53 under varying electric loading and constant compressive stress or under compressive loading-unloading with biased constant electric field clearly demonstrates that the deformation of PZT-53 is volume conservative [11].

### 3.3. Effect of loading history

Following each of the loading cycles (i.e. B–E shown in Fig. 5), the specimen was imposed to an electric field loading of magnitude 1.56 kV/mm with zero compressive stress (as marked as  $I_E, II_E, III_E$ , and  $IV_E$ ) and followed by mechanical loading and unloading in the range of 0 and  $-120$  MPa with zero electrical field (as marked as  $I_\sigma, II_\sigma, III_\sigma$ , and  $IV_\sigma$ ). Such elaborated loading sequence (see, Fig. 7) is used to investigate how the loading history affects the response of PZT-53 to subsequent loading.

The recorded response can then be used to reveal the effect of loading history upon the response of PZT-53 (see,

Fig. 8 on the corresponding  $E_3 - P_3$  and  $E_3 - \varepsilon_{33}$  curves with zero compressive stress). It is seen that the repeatability of the measured curves is excellent except for the case marked as  $I_E$ . The discrepancy at low field can be explained as follows. At low electric field, the polarization or depolarization is not fully completed (Fig. 5b). As a result, its initial state may vary, resulting in a different initial response. Nevertheless, the shape and size of these curves are very similar. Same finding can be drawn from Fig. 9 for the  $P_3 - \sigma_{33}$  and  $\varepsilon_{33} - \sigma_{33}$  curves of PZT-53 when the electric field was reduced to zero and the specimen was loaded by uniaxial compressive stress during the loading interval shown in Fig. 5. Obtained  $P_3 - \sigma_{33}$  and  $\varepsilon_{33} - \sigma_{33}$  curves reveal that the polarization begins to switch and the sample shows nonlinear deformation when the stress exceeds  $-10$  MPa. After unloading from  $-120$  MPa, the domains only partially switch back, resulting in large remanent strain and polarization. Note that Cao and Evans [12] and Fang and Li [16] obtained similar findings. It can be concluded from Figs 8 and 9 that the loading history has negligible effect upon the material behavior PZT-53, provided that it is free of damage.

## 4. Conclusions

The effect of compressive pre-stress, biased constant electric field and loading history on the electromechanical behavior of a soft ferroelectric ceramic PZT-53 is investigated in this study. It is found that the compressive pre-

stress and constant electric field have a significant effect on their electromechanical properties whilst the effect of loading history is comparably small. The results are useful for a further systematic study, both experimentally and theoretically, of the constitutive behavior of ferroelectric ceramics.

### Acknowledgments

This work is supported by the Natural Science Foundation of China (No. 90205030, 10472088, 10425210) and Ministry of Education of China.

### References

1. J. HERBERT, in "Ferroelectric transducers and sensors Gordon and Breach" (New York, 1982).
2. R. E. NEWNHAM, Q. C. XU and S. DUMAR, *Ferroelectrics* **102** (1990) 77.
3. I. CHOPRA, in "SPIE Proceedings" (Bellingham, Washington, 1995).
4. H. H. A. KRUEGER, *J. Acoust. Soc. Am.* **42** (1967) 636.
5. *Idem.*, *ibid.* **42** (1968) 385.
6. H. H. A. KRUEGER and D. BERLINCOURT, *ibid.* **33** (1961) 1399.
7. Z. G. SUO, C. M. KUO and D. M. BARNETT *et al.*, *J. Mech. Phys. Solids* **40** (1992) 739.
8. S. C. HWANG, S. C. LYNCH and R. M. MCMEEKING, *Acta Mater.* **43** (1995) 2073.
9. S. C. HWANG, J. E. HUBER, R. M. MCMEEKING *et al.*, *J. Appl. Phys.* **84** (1998) 1530.
10. D. Y. ZHOU, M. K. KAMLAH and D. MUNZ, *J. Euro. Ceram. Soc.* **25** (2005) 425.
11. C. S. LYNCH, *Acta Mater.* **44** (1996) 4137.
12. H. CAO and A. G. EVANS, *J. Am. Ceram. Soc.* **76** (1993) 890.
13. A. B. SCHAUFLELE and K. H. HARDTL, *ibid.* **79** (1996) 2637.
14. W. CHEN and C. S. LYNCH, *J. Eng. Mater. Tech.* **123** (2001) 169.
15. J. E. HUBER and N. A. FLECK, *J. Mech. Phys. Solids.* **49** (2001) 785.
16. D. N. FANG and C. Q. LI, *J. Mater. Sci.* **34** (1999) 4001.
17. D. VIEHLAND and Y. H. CHEN, *J. Appl. Phys.* **88** (2000) 6696.
18. J. SHIEH, J. E. HUBER and N. A. FLECK, *Acta Mater.* **51** (2003) 6123.

Received 25 March 2004  
and accepted 9 May 2005